Design of an injectable synthetic and biodegradable surgical biomaterial

Peter N. Zawaneh[a], Sunil P. Singh[b], Robert F. Padera[c], Peter W. Henderson[b], Jason A. Spector[b], and David Putnam[a,d,1]

[a]School of Chemical and Biomolecular Engineering and [d]Department of Biomedical Engineering, Cornell University, Ithaca, NY 14853; [b]Weill Cornell Medical College, New York, NY 10065; and [c]Department of Pathology, Brigham and Women's Hospital, Boston, MA 02115

Edited* by Robert Langer, Massachusetts Institute of Technology, Cambridge, MA, and approved April 26, 2010 (received for review November 12, 2008)

We report the design of an injectable synthetic and biodegradable polymeric biomaterial comprised of polyethylene glycol and a polycarbonate of dihydroxyacetone (MPEG-pDHA). MPEG-pDHA is a thixotropic physically cross-linked hydrogel, displays rapid chain relaxation, is easily extruded through narrow-gauge needles, biodegrades into inert products, and is well tolerated by soft tissues. We demonstrate the clinical utility of MPEG-pDHA in the prevention of seroma, a common postoperative complication following ablative and reconstructive surgeries, in an animal model of radical breast mastectomy. This polymer holds significant promise for clinical applicability in a host of surgical procedures ranging from cosmetic surgery to cancer resection.

hydrogel | seroma prevention | dihydroxyacetone | surgical biomaterial

Polymeric biomaterials have contributed significantly to the advancement of medical and surgical practice over the past few decades. Their macromolecular structure can be tailored to provide the appropriate combination of chemical, physical, and biological properties necessary for a range of medical and surgical applications. The rational design of polymeric biomaterials has impacted many fields, including drug and gene delivery, orthopedics, tissue engineering, ophthalmology, and general surgery (1–3). The work reported herein focuses on the development of an injectable surgical biomaterial. Its potential impact is demonstrated in the prevention of postoperative seroma.

A seroma is an abnormal collection of serous fluid within the tissues of the body, akin to an internal blister. Seroma formation is a common postoperative complication particularly following ablative and reconstructive surgeries. Surgeries that require extensive tissue dissection and create large empty spaces can disrupt normal lymphatic flow. Subsequently, transduate fluid collects in these poorly drained "dead spaces," resulting in formation of a seroma (4, 5). Seromas can lead to significant patient morbidity, such as infection, decreased limb mobility, and reoperation (4, 6, 7). Seroma formation rates range from 9.1% to 81%, depending on the nature of the surgical procedure (6, 8–13). Notably, modified radical mastectomies lead to seroma formation rates ranging from 15% to 38.6%, and radical mastectomies report a rate as high as 52% (7, 14–17). In current clinical practice, silicone surgical drains are placed in the wound bed through separate stab incisions to collect transudate fluid, but they can be a significant source of pain and discomfort to patients, especially upon their removal up to several weeks after the initial surgical procedure. Furthermore, they can increase the risk of infection at the surgical site.

Several approaches to reduce seroma formation have been investigated. Surgical techniques, such as collapsing the seroma cavity with sutures, do not consistently and adequately eliminate seroma formation (16, 18, 19). Other methods, such as sclerotherapy (20, 21), compression dressings (22), and biological adhesives, particularly fibrin glue (23–27), have not significantly decreased the clinical incidence of seroma formation.

A more promising, and underexplored, approach involves the application of synthetic biomaterials to eliminate dead space and reduce seroma formation. To date, only two biomaterials, a photopolymerizable polyethylene oxide (28) and a sprayable polyurethane (29), have been previously reported.

Therefore, the current state of postoperative seroma prevention prompted our interest in the design of a surgical biomaterial with adjustable physiochemical properties that is biocompatible, easy to handle and apply, and capable of preventing postoperative seromas. Subsequently, a design strategy that bridges the fields of polymer chemistry, polymer physics and medicine was adopted. We have previously described the successful synthesis and characterization of a diblock copolymer, MPEG-pDHA, comprised of a monomethoxy poly(ethylene glycol) (MPEG) block, and a polycarbonate (pDHA) block based on the metabolic intermediate, dihydroxyacetone (DHA) (30). Our present paper describes the characterization of an MPEG-pDHA-based physically cross-linked hydrogel that is thixotropic, displays rapid chain relaxation, possesses high porosity and high water content, and whose physical and rheological properties can be fine-tuned by adjusting the length of its constituting blocks. This biomaterial degrades into biocompatible products, displays good in vivo biocompatibility, and, most importantly, successfully eliminates seroma formation in an animal model of radical mastectomy.

Results and Discussion

There is an unmet clinical need for the development of effective seroma preventatives. Surprisingly, there are only two published accounts of synthetic biomaterials for seroma prevention (28, 29). Silverman et al. (28) reported a photopolymerizable material that effectively reduced seroma in a rat mastectomy model, but no follow on studies have been reported. Rubin and coworkers (29) have developed a urethane-based material that shows efficacy in a dog seroma model. However, though the results are promising, the material requires long cure times and appears to be slowly degradable. Given that seromas cause significant patient morbidity, it is interesting that they have not received more attention from the biomaterials community.

The design strategy and results presented in this paper describe a diblock copolymer of monomethoxy-polyethylene glycol and a polycarbonate based on the human metabolite dihydroxyacetone (MPEG-pDHA) and its ability to prevent postoperative seroma.

PEG-based polymers have received considerable attention as biomaterials owing to PEG's favorable chemical and biological properties, particularly its established biocompatibility and low immunogenicity (31). DHA is a three-carbon ketose that is an intermediate metabolite in the glycolysis pathway, making it a promising building block for new biomaterials (32). Additionally, DHA is readily manufactured as a fermentative product from corn syrup and methanol (33). It is currently used as the active

Author contributions: P.N.Z., J.A.S., and D.P. designed research; P.N.Z., S.P.S., P.W.H., and J.A.S. performed research; P.N.Z. and R.F.P. analyzed data; and P.N.Z. and D.P. wrote the paper.

The authors declare no conflict of interest.

*This Direct Submission article had a prearranged editor.

[1]To whom correspondence should be addressed. E-mail: dap43@cornell.edu.

This article contains supporting information online at www.pnas.org/lookup/suppl/doi:10.1073/pnas.0811529107/-/DCSupplemental.

www.pnas.org/cgi/doi/10.1073/pnas.0811529107

ingredient in sunless tanning lotions owing to its ability to form Schiff bases by the reaction of primary amines with its C2 carbonyl (34–36). The DHA-based polycarbonate (pDHA) is hydrophilic, but insoluble in water and most common organic solvents, and is also amendable to one-step functionalization through reductive amination at the C2 carbonyl group (37). The MPEG-pDHA diblock copolymer captures some of the properties of both its constituting blocks and incorporates them to form a physically cross-linked hydrogel upon hydration. Our working hypothesis was that MPEG-pDHA-based hydrogels could be injected into the wound bed to act as both a space filler and bioadhesive, owing to pDHA's capacity to bind primary amines (37), allowing the gel to hold the tissue flaps together and seal surrounding leaky blood vessels and lymphatics, thereby reducing fluid accumulation.

The properties and performance of the gel can be controlled by adjusting the length of the polymer's constituting blocks. Subsequently, MPEG-pDHA was synthesized in three different molecular weights (M_w). The MPEG M_w was held constant at 5,000 because at this low M_w, it can undergo renal clearance and is FDA approved for human use. The pDHA M_w was varied (3,000, 5,000, and 7,000) to produce the three desired block copolymers (abbreviated as 5,000–3,000, 5,000–5,000, and 5,000–7,000). MPEG is a water-soluble hydrophilic polymer, whereas pDHA is insoluble in water but hydrophilic based on contact angle measurements (37). These characteristics allow the block copolymers to form nanoparticles at low concentrations in aqueous environments (30). At higher polymer concentrations, the block copolymers form gels with physically entangled networks. Such physical gelation has been observed previously with gels of multiblock copolymers in selective solvents (38–41).

The increase in the pDHA chain length increases the size of the insoluble pDHA domains that form the physical cross-links of the gel, and reduces the relative contribution of the hydrophilic MPEG domain (38). This subsequently increases the entanglement density (Table 1), which in turn influences the gel porosity and water uptake. High water content and increased porosity tend to improve a material's biocompatibility, and can also influence its viscosity and elastic nature (1). The MPEG-pDHA gels exhibit a high water content that decreases with increasing pDHA chain length and entanglement density, as shown in Table 1. The scanning electron micrographs (SEMs) of cryogenically frozen/lyophilized gels shown in Fig. 1 also illustrate a high degree of porosity that decreases with increasing pDHA chain length and entanglement density.

The MPEG-pDHA hydrogels are thixotropic and exhibit a trend of decreasing viscosities with increasing shear rates (Fig. 2*A*). This thixotropic nature allows the hydrogels to form extrudable materials that can be delivered to the seroma by injection even at remote sites. An increase in the pDHA chain length and subsequent increase in entanglement density lead to an increase in hydrogel viscosity (Fig. 2*A*). Figure 2*B* illustrates an example of MPEG-pDHA 5,000–5,000 upon extrusion from a narrow-bore 26-gauge hypodermic needle. The complete set of viscosity measurements at 28 and 37 °C is provided in *SI Text*.

Controlling the hydrogel's entanglement density is essential for controlling its viscosity and porosity. Entanglement densities (Table 1) are calculated from the storage (G′) and loss (G″) moduli measurements (as detailed in *Materials and Methods*), which also provide insight into the elastic nature of the gels. Figure 2*C* is an example of a typical G′ and G″ graph as obtained for the MPEG-pDHA hydrogel (5,000–3,000 and 5,000–7,000). The G′ values display very low-frequency dependence and are greater than G″ values across the entire frequency range, a trend characteristic of elastic hydrogels (42, 43). The G′ and G″ values also increase with increasing pDHA chain length and entanglement density. The complete set of G′ and G″ measurements is provided in *SI Text*.

The MPEG-pDHA chain relaxation time was calculated from the rheological data. Relaxation calculations help determine the hydrogel relaxation kinetics following a step strain, which can provide insight into how long it takes the MPEG-pDHA hydrogel chains to relax to their equilibrium state following injection at the seroma site. Rapid relaxation times help ensure that a biomaterial rapidly reverts to its equilibrium state, and subsequently reduce the number of variables that can influence the performance of a therapeutic hydrogel in vivo. The MPEG-pDHA gels display rapid relaxation times (250–350 s), which also increase with increasing pDHA chain length and entanglement density (Table 1) (44). *Materials and Methods* includes the equations that were used to calculate the MPEG-pDHA hydrogel relaxation times. The complete set of chain relaxation data is provided in *SI Text*.

Two important characteristics for new biomaterials are the rate of degradation and the composition of the degradation products. The in vitro degradation studies performed on the MPEG-pDHA block copolymers indicate that degradation rates are surprisingly rapid for a polycarbonate and decrease with increasing pDHA block M_w, but all copolymers degrade to completion in 24 h (Fig. 3*A*). Figure 3*B* is a characteristic ^{1}H NMR of the block copolymer degradation products, which shows that the soluble polymer degradation products are MPEG, monomeric DHA, and presumably CO_2 (CO_2 is a common byproduct of polycarbonate degradation) (45, 46). As a reference, *SI Text* includes ^{1}H NMRs of neat MPEG and DHA, respectively. A comparison of Fig. 3 and the corresponding *SI Text* figure shows that the ^{1}H NMR peaks overlap, indicating that the degradation products of MPEG-pDHA are MPEG and monomeric DHA.

Following the rheological and degradation characterization of MPEG-pDHA, we evaluated how the hydrogel performed in a potential surgical application, the prevention of postoperative seroma. A well-established rat mastectomy model was used to determine the efficacy of MPEG-pDHA, and to allow direct comparison with the literature (28). As shown in Fig. 4, the untreated controls displayed a mean seroma volume of 2.28 ± 0.55 mL, whereas MPEG-pDHA 5,000- to 3,000-treated rats displayed a significantly decreased mean seroma volume of 0.044 ± 0.017 mL ($P < 0.01$). Interestingly, MPEG-pDHA 5,000- to 5,000- and 5,000- to 7,000-treated rats displayed a mean seroma volume of 2.53 ± 0.70 ($P = 0.8$) and 1.93 ± 0.60 ($P = 0.2$), respectively, which is statistically equivalent to the untreated control animals. Post-

Table 1. Summary of MPEG-pDHA gel swelling characteristics, cross-link density, and chain relaxation times following shear

Sample MPEG-pDHA	Weight gain swelling, %	Entanglement density ν, m^{-3}	Relaxation time τ, s
5,000–3,000	587.5 ± 18.3	4.96e24	250
5,000–5,000	513.1 ± 12.2	1.48e25	250
5,000–7,000	396.0 ± 22.3	3.25e25	350

Increasing the pDHA chain length reduces the extent of swelling and increases the hydrogel cross-link density and relaxation time.

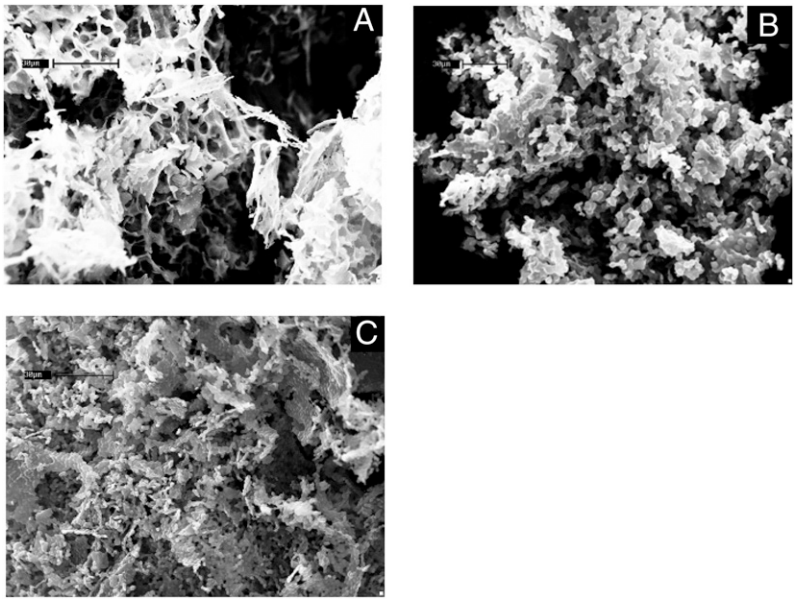

Fig. 1. SEMs of lyophilized MPEG-pDHA gels. (*A*) 5,000–3,000. (*B*) 5,000–5,000. (*C*) 5,000–7,000. Increasing the pDHA chain length reduces the hydrogel porosity.

mortem examination of animals treated with MPEG-pDHA 5,000–3,000 showed gross fibrinous adhesions between the elevated skin flap and chest wall, whereas no adhesions were evident in the other treatment or control groups. In vivo degradation of the polymer was confirmed by the absence of residual polymer (all three compositions) upon histological examination of excised tissue from the wound bed at 7 days after application. At day 1 postsurgery, residual MPEG-pDHA was evident (*SI Text*), suggesting the in vivo rate of degradation is slower than observed in vitro; however, no residual polymer was visualized on day 3 (*SI Text*).

To make a correlation between antiseroma efficacy and the polymer structure, we conducted three mechanism-oriented experiments. First, we degraded MPEG-pDHA 5,000–3,000 in water into oligomeric products to ascertain whether the polymer degradation products were a causative factor in seroma prevention. As shown in Fig. 4, hydrolyzed MPEG-pDHA was ineffective, suggesting the full-length polymer upon administration

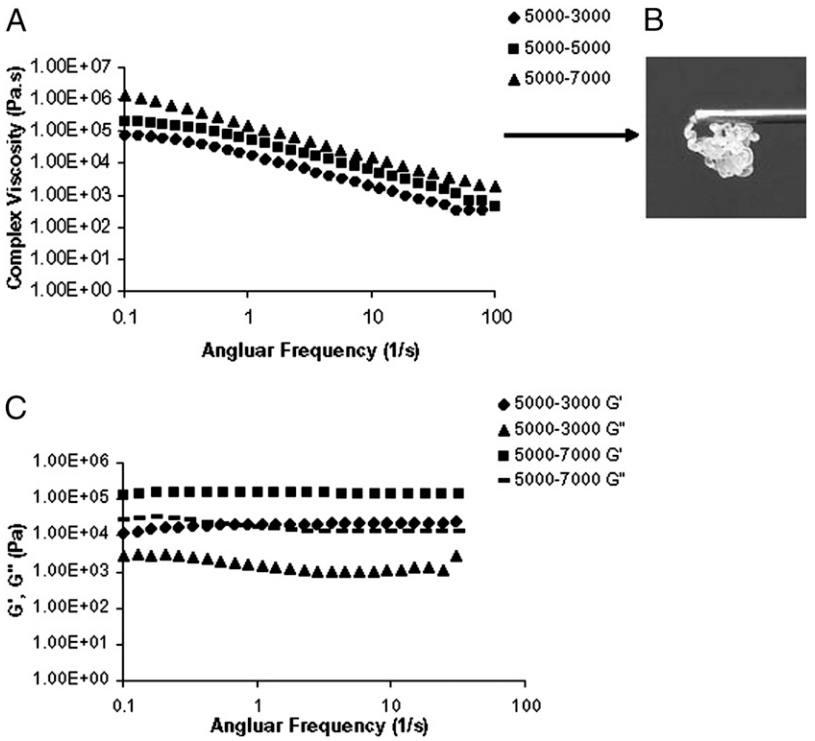

Fig. 2. (*A*) Viscosity readings show the MPEG-pDHA hydrogel thixotropic behavior (1% strain, 28 °C). (*B*) An example of MPEG-pDHA 5,000–5,000 extruded from a 26-gauge needle. (*C*) G′ and G′′ readings as obtained from frequency sweep experiments on the MPEG-pDHA gels (1% strain, 28 °C).

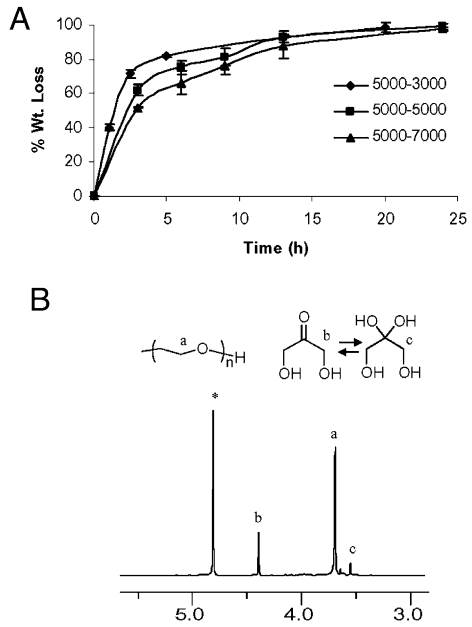

Fig. 3. (*A*) Kinetics of weight loss of MPEG-pDHA hydrogels in water show 100% degradation within 1 day. (*B*) ^{1}H NMR of hydrolyzed MPEG-pDHA products in D_2O, indicate that the end products are MPEG and monomeric DHA.

is necessary for antiseroma activity. Second, the MPEG-pDHA hydrogel was hydrated in the presence of a twofold mole excess of lysine (relative to C2 carbonyl groups) to determine whether the C2 carbonyl reactivity with the primary amines in the tissue was necessary for antiseroma activity. The lysine was added to occupy the C2 carbonyl groups; therefore, if C2 reactivity with the amines in the tissue is necessary for activity, the lysine-hydrated formulation should be less active. As shown in Fig. 4, although the lysine-hydrated formulation showed a reduced seroma volume, the reduction was statistically equivalent to the control, suggesting that the reactivity of the C2 carbonyl takes part in preventing seroma. Third, to determine if MPEG-pDHA initiated the clotting cascade to facilitate tissue integration, we measured the effect of the polymer on prothrombin time (PT) and partial thromboplastin time (PTT). The findings, reported in a study that focuses on the hemostatic capabilities of MPEG-pDHA, show that biomaterial has no effect on PT and PTT, suggesting that activation of the clotting cascade is not a factor in seroma prevention (47).

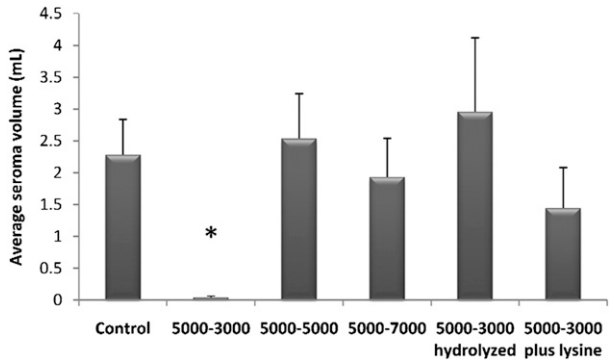

Fig. 4. Seroma volumes from a rat mastectomy model. The untreated controls displayed a mean seroma volume of 2.28 ± 0.55 mL (n = 6). MPEG-pDHA 5,000- to 3,000-treated rats displayed a mean seroma volume of 0.044 ± 0.017 mL (n = 9, $P < 0.01$). MPEG-pDHA 5,000- to 5,000-treated rats displayed a mean seroma volume of 2.53 ± 0.70 (n = 8). MPEG-pDHA 5,000- to 7,000-treated rats had a mean seroma volume of 1.93 ± 0.60 (n = 8). Treatment with both hydrolyzed and lysine-treated MPEG-pDHA did not result in statistically significant reduction in seroma volume relative to untreated control (2.6 ± 1.16, n = 6, and 1.41 ± 0.63, n = 6, respectively).

With respect to biocompatibility, there was normal-appearing early granulation tissue and a mild inflammatory response that was equal to untreated control animals (Fig. 5). These findings suggest that MPEG-pDHA and its degradation products are well tolerated by the soft tissue surrounding the wound bed and do not negatively impact the normal sequence of early wound healing.

Collectively, these data demonstrate MPEG-pDHA's potential as a highly effective surgical biomaterial. Given its ease of delivery (injection), compatibility with living tissue, and in vivo efficacy, MPEG-pDHA may hold significant clinical utility for the prevention or treatment of postoperative seroma.

Materials and Methods

Materials. MPEG (M_w 5000) was purchased from Polysciences. Before use, MPEG was dried by azeotropic distillation in toluene. DHA, *p*-toluene sulfonic acid, trimethyl orthoformate, $Sn(Oct)_2$, ethyl chloroformate, and 5% phosphotungstic acid were purchased from Sigma-Aldrich and used as received. Triethylamine, tetrahydrofuran (THF), dichloromethane (CH_2Cl_2), diethyl ether, methanol, toluene, and TFA were purchased from VWR and used as received. Syringes and PBS (pH 7.4) were purchased from Fisher Scientific. Collagen was purchased from MP Biomedicals.

Equipment. ^{1}H NMR spectra were recorded on a Mercury 300 spectrometer. Gel permeation chromatography (GPC) was carried out using PSS SDV columns 500A, 50A, and linear M (in series) with a THF mobile phase (1 mL/min) and polystyrene standards with UV (Waters 486) and RI (Waters 2410) detection. Rheology measurements were performed using a Physica Modular Compact 300 Rheometer. Scanning electron microscopy measurements were performed using the Leica 440.

Polymer Synthesis. Poly(MPEG-b-2-oxypropylene carbonate) (VII; MPEG-pDHA) was synthesized using a previously published protocol developed in our lab (30). Briefly, dihydroxyacetone dimer (II) was locked in its monomeric form by conversion of its C2 carbonyl group into a dimethoxy acetal using trimethyl-orthoformate and *p*-toluenesulfonic acid (III). This was then converted to a six-membered cyclic carbonate (IV). IV was polymerized using Sn $(Oct)_2$ in the presence of monomethoxy poly(ethylene glycol) (MPEG) to form VI. The molecular weight of the MPEG was fixed at 5,000, whereas the molecular weight of the DHA-based polymer chain was varied depending on the reactant feed ratios and the $Sn(Oct)_2$ injection conditions (molecular weights of 3,000, 5,000, 7,000, and 10,000 were synthesized). This polymer was subsequently deprotected using a TFA water mixture (4:1) to produce the desired polymer, MPEG-pDHA (VII). The amount of TFA water needed to deprotect the polymer depended on the length of the pDHA-based segment. *SI Text* summarizes the polymerization conditions used to synthesize each molecular weight. The reaction scheme is also shown in *SI Text*. MPEG-pDHA ^{1}H NMR (DMSO-d_6) δ: 5.00 (s; 4H), 3.50 (s; 4H), 3.24 (s; 3H).

Hydrogel Characterization. The swelling degree was obtained by hydrating 30 mg of each MPEG-pDHA molecular weight (n = 4) in 1.0 mL of PBS at room temperature. The gels were allowed to sit for ≈4 min on a filter paper to drain the excess PBS. The gels were weighed to obtain the swollen weight (W_s), then lyophilized and weighed again to obtain the dry weight (W_d). Swelling degree was calculated using Eq. **1** (48):

$$\text{swelling degree } (\%) = (Ws/Wd)*100 \qquad [1]$$

Rheological tests were performed using a Physica Modular Compact 300 using parallel plate geometry (8-mm diameter parallel plate). Data were recorded using US200 software and analyzed using an Excel spreadsheet. All experiments were performed at 28 °C and 37 °C. The viscoelastic properties of the gels were determined by performing frequency sweep experiments in the oscillatory mode with a 1% strain amplitude and frequency range of 0.1 to 100 1/s. Step-stain experiments, with a 1% strain, were performed to determine the stress relaxation of the gels.

Entanglement density was calculated using the plateau storage modulus, G_e (the maximum G′ where G′/G″ > 1) (49, 50). Using Eq. **2**:

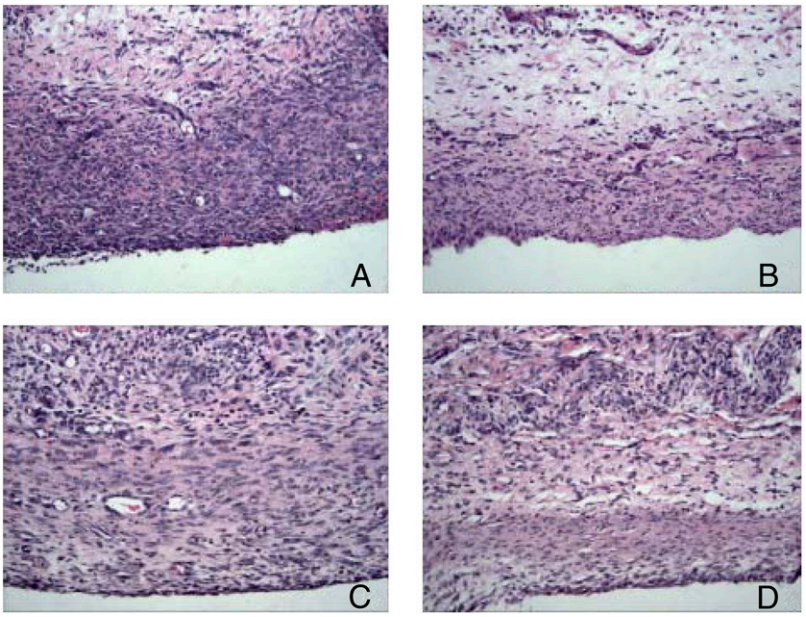

Fig. 5. Light microscopic appearance of surgical sites at 7 days. (*A*) control. (*B*) MPEG-pDHA 5,000–3,000. (*C*) MPEG-pDHA 5,000–5,000. (*D*) MPEG-pDHA 5,000–7,000. The sections show early granulation tissue adjacent to surgical site, which is the clear space at the bottom of all images. (Magnification: H&E stain, 100×).

$$G_e = \nu kT, \qquad [2]$$

where G_e is the plateau G′, ν is the entanglement density (m^{-3}), k is the Boltzman constant ($kg{\cdot}m^2{\cdot}s^{-2}{\cdot}K^{-1}$), and T is the temperature (K).

Calculation of the chain relaxation time (τ) was obtained my measuring the relaxation modulus [G(t)] following a small step strain (as shown in *SI Text*). Using Eq. **3** (49, 50),

$$G\left(t\right) = G\left(\tau\right)\exp^{-t/\tau}, \qquad [3]$$

where G(t) is the relaxation modulus (Pa), G(τ) is constant (Pa), t is time (s), and τ is the chain relaxation time (s).

Differentiating and rearranging Eq. **3** yields:

$$\left[tG(t)\right]' = G\exp^{-\left(\frac{t}{\tau}\right)}\left(1-\frac{t}{\tau}\right). \qquad [4]$$

Using Eq. **4**, a plot of tG(t) vs. t yields a plot with a maximum at t = τ, which is the chain relaxation time (τ).

Hydrolytic Degradation. In vitro degradation studies were performed on MPEG-pDHA 5,000–3,000, 5,000–5,000, and 5,000–7,000. The polymer samples were weighed out into 20-mg samples and placed in 1.0 mL PBS (pH 7.4), 1.5-mL Eppendorf tubes. The samples were placed on an orbital shaker and incubated at 37 °C. Samples were recovered for each polymer at the selected time points (n = 3). The samples were recovered, washed with DI water, lyophilized, and reweighed. Degradation products from fully degraded samples were characterized by ^{1}H NMR. ^{1}H NMR (D_2O) DHA δ: 4.40 (s; 4H), 3.55 (s; 6H). ^{1}H MPEG (D_2O) DHA δ: 3.70 (s; 4H).

Antiseroma Efficacy. To evaluate the efficacy of the polymer gels, each MPEG-pDHA-based gel was evaluated in a well-established rat model of seroma formation (23). Briefly, following a midline incision, a skin flap was raised over the right chest, exposing the right pectorals major muscle, which was then excised. A right axillary lymphadenctomy was then performed under an operating microscope. The fully hydrated hydrogel was prepared freshly to full hydration by mixing 100 mg of lyophilized MPEG-pDHA powder with sterile saline over filter paper. Experimental rats received 0.5 mL of MPEG-pDHA hydrogel into the wound bed before closure, and controls received 0.5 mL of saline into the wound bed before closure.

Animals were killed on postoperative day 7 by carbon dioxide asphyxiation followed by cervical dislocation as per institutional guidelines approved for this investigation. Seroma fluid was aspirated percutaneously via an 18-gauge needle and measured volumetrically. The incision site was then opened, and any remaining seroma fluid was removed by needle aspiration. To determine in vivo biocompatibility of the polymer, sections of the skin flap and the underlying wound bed were removed en bloc and analyzed histologically (H+E stain) for evidence of residual polymer and inflammation in the area of application. A Student two-tailed t test with unequal variance was performed to determine the P value (α = 0.05).

ACKNOWLEDGMENTS. This research was supported in part from a National Science Foundation CAREER Award, a grant from the Morgan Tissue Engineering Fund, an Early Career Award from the Wallace H. Coulter Foundation, and the New York State Center for Advanced Technology.

1. Langer R, Tirrell DA (2004) Designing materials for biology and medicine. *Nature* 428: 487–492.
2. Putnam D (2006) Polymers for gene delivery across length scales. *Nat Mater* 5: 439–451.
3. Wong SY, Pelet JM, Putnam D (2007) Polymer systems for gene delivery-past, present, and future. *Prog Polym Sci* 32:799–837.
4. Agrawal A, Ayantunde AA, Cheung KL (2006) Concepts of seroma formation and prevention in breast cancer surgery. *ANZ J Surg* 76:1088–1095.
5. Kuroi K, et al. (2005) Pathophysiology of seroma in breast cancer. *Breast Cancer* 12: 288–293.
6. Schwabegger A, Ninković M, Brenner E, Anderl H (1997) Seroma as a common donor site morbidity after harvesting the latissimus dorsi flap: Observations on cause and prevention. *Ann Plast Surg* 38:594–597.
7. Budd DC, Cochran RC, Sturtz DL, Fouty WJ, Jr. (1978) Surgical morbidity after mastectomy operations. *Am J Surg* 135:218–220.
8. Woodworth PA, McBoyle MF, Helmer SD, Beamer RL (2000) Seroma formation after breast cancer surgery: Incidence and predicting factors. *Am Surg* 66:444–450, discussion 450–451.
9. Roses DF, Brooks AD, Harris MN, Shapiro RL, Mitnick J (1999) Complications of level I and II axillary dissection in the treatment of carcinoma of the breast. *Ann Surg* 230: 194–201.
10. Abe M, Iwase T, Takeuchi T, Murai H, Miura S (1998) A randomized controlled trial on the prevention of seroma after partial or total mastectomy and axillary lymph node dissection. *Breast Cancer* 5:67–69.
11. Say CC, Donegan W (1974) A biostatistical evaluation of complications from mastectomy. *Surg Gynecol Obstet* 138:370–376.
12. Alvandi RY, Solomon MJ, Renwick SB, Donovan JK (1991) Preliminary results of conservative treatment of early breast cancer with axillary dissection and post operative radiotherapy. A retrospective review of 107 patients. *Aust N Z J Surg* 61: 670–674.

13. Osteen RT, Karnell LH (1994) The National Cancer Data Base report on breast cancer. *Cancer* 73:1994–2000.
14. Hayes JA, Bryan RM (1984) Wound healing following mastectomy. *Aust N Z J Surg* 54: 25–27.
15. Aitken DR, Hunsaker R, James AG (1984) Prevention of seromas following mastectomy and axillary dissection. *Surg Gynecol Obstet* 158:327–330.
16. Chilson TR, Chan FD, Lonser RR, Wu TM, Aitken DR (1992) Seroma prevention after modified radical mastectomy. *Am Surg* 58:750–754.
17. Terrell GS, Singer JA (1992) Axillary versus combined axillary and pectoral drainage after modified radical mastectomy. *Surg Gynecol Obstet* 175:437–440.
18. O'Dwyer PJ, O'Higgins NJ, James AG (1991) Effect of closing dead space on incidence of seroma after mastectomy. *Surg Gynecol Obstet* 172:55–56.
19. Coveney EC, O'Dwyer PJ, Geraghty JG, O'Higgins NJ (1993) Effect of closing dead space on seroma formation after mastectomy—a prospective randomized clinical trial. *Eur J Surg Oncol* 19:143–146.
20. Tekin E, Kocdor MA, Saydam S, Bora S, Harmancioglu O (2001) Seroma prevention by using *Corynebacterium parvum* in a rat mastectomy model. *Eur Surg Res* 33:245–248.
21. Rice DC, et al. (2000) Intraoperative topical tetracycline sclerotherapy following mastectomy: A prospective, randomized trial. *J Surg Oncol* 73:224–227.
22. O'Hea BJ, Ho MN, Petrek JA (1999) External compression dressing versus standard dressing after axillary lymphadenectomy. *Am J Surg* 177:450–453.
23. Lindsey WH, Masterson TM, Spotnitz WD, Wilhelm MC, Morgan RF (1990) Seroma prevention using fibrin glue in a rat mastectomy model. *Arch Surg* 125:305–307.
24. Harada RN, Pressler VM, McNamara JJ (1992) Fibrin glue reduces seroma formation in the rat after mastectomy. *Surg Gynecol Obstet* 175:450–454.
25. Wang JY, et al. (1996) Seroma prevention in a rat mastectomy model: Use of a light-activated fibrin sealant. *Ann Plast Surg* 37:400–405.
26. Sanders RP, et al. (1996) Effect of fibrinogen and thrombin concentrations on mastectomy seroma prevention. *J Surg Res* 61:65–70.
27. Carless PA, Henry DA (2006) Systematic review and meta-analysis of the use of fibrin sealant to prevent seroma formation after breast cancer surgery. *Br J Surg* 93: 810–819.
28. Silverman RP, et al. (1999) Transdermal photopolymerized adhesive for seroma prevention. *Plast Reconstr Surg* 103:531–535.
29. Gilbert TW, et al. (2008) Lysine-derived urethane surgical adhesive prevents seroma formation in a canine abdominoplasty model. *Plast Reconstr Surg* 122:95–102.
30. Zawaneh PN, Doody AM, Zelikin AN, Putnam D (2006) Diblock copolymers based on dihydroxyacetone and ethylene glycol: Synthesis, characterization, and nanoparticle formulation. *Biomacromolecules* 7:3245–3251.
31. Hubbell JA (1998) Synthetic biodegradable polymers for tissue engineering and drug delivery. *Curr Opin Solid State Mater Sci* 3:246–251.
32. Mathews C, Van Holde K (1996) *Biochemistry* (Benjamin/Cummings, Menlo Park, CA).
33. Kato N, Kobayashi H, Shimao M, Sakazawa C (1986) Dihydroxyacetone production from methanol by a dihydroxyacetone kinase deficient mutant of hansenula-polymorpha. *Appl Microbiol Biotechnol* 23:180–186.
34. Soler C, Soley M (1993) Rapid and delayed effects of epidermal growth factor on gluconeogenesis. *Biochem J* 294:865–872.
35. Davis L (1973) Structure of dihydroxyacetone in solution. *Bioorg Chem* 2:197–201.
36. Nguyen BC, Kochevar IE (2003) Influence of hydration on dihydroxyacetone-induced pigmentation of stratum corneum. *J Invest Dermatol* 120:655–661.
37. Zelikin AN, Zawaneh PN, Putnam D (2006) A functionalizable biomaterial based on dihydroxyacetone, an intermediate of glucose metabolism. *Biomacromolecules* 7: 3239–3244.
38. Wang LW, Venkatraman S, Gan LH, Kleiner L (2005) Structure formation in injectable poly(lactide-co-glycolide) depots. II. Nature of the gel. *J Biomed Mater Res B Appl Biomater* 72B:215–222.
39. Nyrkova IA, Khokhlov AR, Doi M (1993) Microdomains in block copolymers and multiplets in ionomers: Parallels in behavior. *Macromolecules* 26:3601–3610.
40. He XW, Herz J, Guenet JM (1988) Physical gelation of a multiblock copolymer: Effect of copolymer composition. *Macromolecules* 21:1757–1763.
41. He XW, Herz J, Guenet JM (1989) Physical gelation of a multiblock copolymer: Effect of solvent type. *Macromolecules* 22:1390–1397.
42. Vermonden T, M NA, van MJ, Hennink WE (2006) Rheological studies of thermosensitive triblock copolymer hydrogels. *Langmuir* 22:10180–10184.
43. Nowak AP, et al. (2002) Rapidly recovering hydrogel scaffolds from self-assembling diblock copolypeptide amphiphiles. *Nature* 417:424–428.
44. Sahiner N, Singh M, De Kee D, John VT, McPherson GL (2006) Rheological characterization of a charged cationic hydrogel network across the gelation boundary. *Polymer (Guildf)* 47:1124–1131.
45. Tangpasuthadol V, Pendharkar SM, Kohn J (2000) Hydrolytic degradation of tyrosine-derived polycarbonates, a class of new biomaterials. Part I: Study of model compounds. *Biomaterials* 21:2371–2378.
46. Zhu KJ, Hendren RW, Jensen K, Pitt CG (1991) Synthesis, properties, and biodegradation of poly(1,3-trimethylene carbonate). *Macromolecules* 24:1736–1740.
47. Henderson PW, et al. (2009) A rapidly resorbable hemostatic biomaterial based on dihydroxyacetone. *J Biomed Mater Res A* 93A:776–782.
48. Barbucci R, Rappuoli R, Borzacchiello A, Ambrosio L (2000) Synthesis, chemical and rheological characterization of new hyaluronic acid-based hydrogels. *J Biomat Sci Polym Ed* 11:383–399.
49. Rubinstein M, Colby R (2003) *Polymer Physics* (Oxford Univ Press, New York).
50. Macosko CW (1994) *Rheology: Principles, Measurements, and Applications* (VCH, New York).